Biomaterials Advances 177 (2025) 214379

Contents lists available at ScienceDirect

Biomaterials Advances

journal homepage: www.journals.elsevier.com/materials-science-and-engineering-c

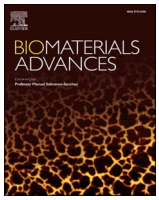

Magnesium and strontium-enriched bioactive glasses: superior biocompatibility and angiogenesis, beyond the gold standard

Marianna Barbalinardo [a,1], Marzia Ferretti [b,1], Virginia Stanzani [b], Francesca Chiarini [b,*], Ilaria Zanoni [c], Francesca Paganelli [d], Marta Checchi [b], Serena Truocchio [d], Matteo Corradini [b], Vincenza Rita Lo Vasco [b], Francesco Cavani [b], Luca Reggiani Bonetti [e], Devis Bellucci [f,*], Valeria Cannillo [f,2], Carla Palumbo [b,2]

[a] Institute for the Study of Nanostructured Materials (CNR-ISMN), National Research Council of Italy, 40129 Bologna, Italy
[b] Department of Biomedical, Metabolic and Neural Sciences, University of Modena and Reggio Emilia, 41124 Modena, Italy
[c] Institute of Science, Technology and Sustainability for Ceramics (CNR-ISSMC), National Research Council of Italy, 48018 Faenza, Italy
[d] Department of Biomedical and Neuromotor Sciences, Alma Mater Studiorum - University of Bologna, 40126 Bologna, Italy
[e] Department of Medical and Surgical Sciences for Children and Adults, University of Modena and Reggio Emilia, 41124 Modena, Italy
[f] Department of Engineering "Enzo Ferrari", University of Modena and Reggio Emilia, 41125 Modena, Italy

ARTICLE INFO

Keywords:
Bioactive glasses
Therapeutic ions
CAM assay
Angiogenesis
Bone tissue engineering

ABSTRACT

Bioactive glasses (BGs) have garnered attention for their potential as transformative bone substitutes in regenerative medicine. BGs exert their effects through the dissolution of active ions that can stimulate osteoprogenitors and endothelial cells in the osteogenic process. In this paper, two recent BGs formulations (BGMS10 and Bio_MS), enriched in Sr and Mg ions and with extremely high crystallization temperature, were evaluated. The effects of such BGs on endothelial cell adhesion, viability, and proliferation were analyzed both in the actual presence of BGs and in indirect settings, to determine the impact of ionic dissolution products. The novel BGs were compared to 45S5 Bioglass®, demonstrating a significantly higher biocompatibility and viability of cells grown onto the two novel formulations. Then, the angiogenic potential was evaluated *via* the Chorio-Allantoic Membrane (CAM) assay which, acting as natural bioreactor, simulates the *in vivo* conditions. All the BGs demonstrated to be significantly pro-angiogenic compared to controls, showing a significant upregulation of genes with a key role in angiogenic pathways. These observations were consistent with the tissue histological evaluations, which displayed high biocompatibility of BGMS10 and Bio_MS, and a remarkable proliferation of CAM tissues with no inflammatory reactions. In conclusion, our results show that these novel formulations are extremely effective in promoting cell adhesion, proliferation and angiogenesis, which are fundamental for the complex process of healing.

1. Introduction

A significant and increasing portion of the world elderly population is affected by musculoskeletal disorders, with estimates of hundreds of millions of people interested and a related increase in the costs of the national health system. Consequently, there is a growing demand for materials that can replace damaged or missing tissues and facilitate the healing process. Autologous or heterologous implants have inherent limitations, such as donor site pain and the risk of pathogens transmission [1–4]. As a result, natural and synthetic materials have been explored as innovative/alternative solutions for tissue engineering and regenerative medicine applications [5].

Among synthetic materials, bioactive glasses (BGs) have shown promising results in bone tissue regeneration [6]. The primary advantage of BGs is their capacity to bond with living tissues, promoting bone growth and regeneration. Additionally, BGs possess antibacterial properties and have been shown to be highly effective in treating bone infections. However, one of the main challenges when using BGs is their

* Corresponding authors.
E-mail addresses: francesca.chiarini@unimore.it (F. Chiarini), devis.bellucci@unimore.it (D. Bellucci).
[1] Contributed equally to this work.
[2] Last, co-last authors.

https://doi.org/10.1016/j.bioadv.2025.214379
Received 12 March 2025; Received in revised form 29 May 2025; Accepted 7 June 2025
Available online 9 June 2025

tendency to crystallize at high temperatures, which can affect their bioactivity, thus limiting their use in the clinical scenario [7]. In fact, due to the preferential degradation of the residual glassy phase by the surrounding biological environment, the resulting sintered parts may crystallize and have reduced bioactivity, causing instability of the implant and eventually be hazardous in clinical settings. Additionally, the regenerative capability of bioactive glasses is greatly influenced by their ionic release, which is essential in angiogenesis and osteogenesis.

Recent studies have also explored innovative strategies for enhancing bioactivity and bone regeneration also using bioglass-based composites [8–11]. These studies further confirm the versatility of bioglasses as key components in regenerative systems, for their osteoconductive and angiogenic roles, and also for their capability to modulate the biological environment, an aspect increasingly recognized as essential for successful bone repair.

It is well known that the angiogenic properties of biomaterials directly influence osteogenesis through mechanisms of angiogenic-osteogenic coupling. However, this process may be delayed in partially crystallized samples [12,13].

To overcome BGs limitations, current research has aimed at modifying the ion composition of BGs to improve their crystallization temperature. By adjusting the concentration of different ions, it is possible to optimize the glass composition to achieve higher crystallization temperatures and stability [14–16]. Moreover, the use of the so-called "therapeutic" ions has shown very positive effects on biological responses [17]. For instance, silicon is known for inducing endothelial cell migration, differentiation and neoblood vessels sprouting, key and essential prerequisites for correct and effective osteogenesis, whereas phosphorus has been shown to induce vascular endothelial growth factor A (VEGF-A) expression, human umbilical vein endothelial cell migration and tube formation [18]. Moreover, calcium and magnesium can stimulate endothelial cell proliferation and migration, increasing different growth factors as VEGF-A and platelet-derived growth factor (PDGF), and enhancing the mitogenic response to angiogenic factors [19].

Here we have analyzed the potential of two novel BGs on endothelial cell adhesion, cell viability and in the vascularization process in *in vitro* and *in vivo* environments. BGMS10 is a new formulation characterized by the addition of strontium and magnesium ions as a promising alternative to the original 45S5 Bioglass®, the gold standard in the field of bioactive glasses [20]. BGMS10 showed an exceptional combination of properties, including a high crystallization temperature of approximately 932 °C, as well as excellent biocompatibility and bioactivity, in *in vitro* testing with human mesenchymal stem cells (MSCs) [21]. Thus, this glass can be employed in a wide range of derivative products, including granules, composite systems, scaffolds, wound dressings, dental putties and coatings. In the same way, another composition containing strontium and magnesium, the Bio_MS BG, demonstrated very promising features, thus exhibiting exceptional biological performance, compared to 45S5 Bioglass®, such as very high crystallization temperature and a wide processing window that allows the production of an amorphous BG, even after thermal treatment. Indeed, Bio_MS has been patented (Italian patent) due to its outstanding performance. Its biological responsiveness was also partly assessed using simulated body fluid (SBF) and bone marrow mesenchymal stem cells (BMSCs), which successfully colonized the material and differentiated into osteogenic lineage cells [22].

However, angiogenesis, a biological process crucial to maintain the natural homeostasis of tissues, is fundamental to induce the bone regenerative processes. In bone, when a severe vascular damage occurs and the natural regenerative capacity is compromised, the restoration of a functional vascular network is a mandatory prerequisite to form a new matrix and to induce osteogenesis. As a result, for an effective healing process, biomaterials must possess angiogenic potential to be suitable for bone tissue regeneration [23]. In this context, the chorio-allantoic membrane (CAM) assay is an effective method for assessing the pro- or anti-angiogenic properties of biomaterials [24,25]. Pro-angiogenic properties can be easily detected because CAM responds with a vascular reaction characterized by vessels of new formation developing radially from the tested material. The CAM assay represents an alternative model to animal experimentation that does not necessitate any approval from ethical committees until the 17th day of embryos development, fully following the Replacement, Reduction and Refinement principle [26].

In this study, we found that BGMS10 and Bio_MS bioglasses displayed significant better performances compared to 45S5 in terms of endothelial cell adhesion, colonization, proliferation and angiogenic potential both *in vitro* and *in vivo*. These results suggest that BGMS10 and Bio_MS bioglasses could be successfully employed in bone tissue engineering applications in a clinical perspective, by harnessing their improved properties resulting from ionic release that enhances cellular adhesion, growth and vascularization.

2. Materials & methods

2.1. Preparation of BG granules

The BG granules discussed in this work were manufactured using a traditional melting technique, which has been thoroughly discussed in previous studies [27]. The composition of the bioactive glasses employed are provided in Table 1. Briefly, the powdered reagents (all reagents grade, Carlo Erba Reagents, Milan, Italy) were mixed for 6 h (h) and then placed in a platinum crucible. The temperature was gradually increased by 10 °C per minute (min) until it reached 1450 °C. Additionally, an isothermal step at 1100 °C was performed for 1 h to facilitate the decarbonation of the reagents. Following this, the molten glass was poured into room temperature (RT) water, resulting in a frit, which was subsequently dried for 24 h at 110 °C. The frits were further processed by grinding and sieving, producing granules (particle size ranging from 250 to 500 μm) for subsequent biological testing. The 45S5 Bioglass® is a commercially available product [5], with characteristic temperatures widely known and documented in literature, whereas BGMS10 and Bio_MS granules have been characterized for their properties in previous studies [20,22].

2.2. Ionic release

The ionic release from the three BGs soaked in Dulbecco's Modified Eagle Medium (DMEM) (Gibco, Thermo Fisher Scientific, Waltham, MA, USA) added with 10 % Fetal Bovine Serum (FBS) (Sigma Aldrich, Darmstadt, Germany), was assessed at 16 and 48 h by inductively coupled plasma (ICP) optical emission spectrometry using an ICP-OES 5100 – vertical dual view apparatus (Agilent Technologies, Santa Clara, CA, USA) coupled with OneNeb nebulizer and equipped with an Autosampler. Argon was selected as the internal standard (wavelength 420 nm). The measurements were calibrated by the use of calibration curves with a correlation coefficient limit higher than 0.999. The calibration fit was linear, including a blank in calibration. The measurements precision for the analysis, indicated as ratio of the standard

Table 1
Composition (in oxides mol%) of the produced glasses.

Oxides	Composition [mol%]		
	45S5 [5]	BGMS10 [20]	Bio_MS [22]
SiO_2	46.1	47.2	46.1
P_2O_5	2.6	2.6	2.6
Na_2O	24.4	2.3	5.0
CaO	26.9	25.6	31.3
K_2O	0	2.3	0
MgO	0	10.0	5.0
SrO	0	10.0	10.0

deviation to the mean (RSD) in percentage, was always <5 %. The limit of detection (LOD) at the operative wavelength was 0.01 mg L^{-1} for Sr, 0.1 mg L^{-1} for Si, and 1 mg L^{-1} for Ca and Mg. In the wavelength selection for elemental analysis, each element wavelength was chosen based on its intensity and possible interferences with the medium. Before each analysis, samples were acid digested, adding 10 % *v*/v of phosphoric acid (H_3PO_4 96 %) and 10 % v/v of hydrogen peroxide (H_2O_2 30 %). Calibration curves were built in the range of 0.01–100.00 μg/mL, using standards prepared in DMEM +10 % FBS medium and applying the same digestive procedure of samples.

2.3. Cell culture

Mouse aortic endothelial cells (MAEC), kindly provided by Prof. Stefania Mitola (University of Brescia, Italy), were cultivated under standard conditions in DMEM (Gibco, Thermo Fisher Scientific, Waltham, MA, USA) completed with 10 % fetal bovine serum (FBS), 2 mM L-glutamine, and 100 U·mL^{-1} penicillin, and 100 U·mL^{-1} streptomycin (all Sigma Aldrich, Darmstadt, Germany) in a humidified incubator set at 37 °C with 5 % CO_2. Before cell seeding, BG granules were subjected to UV light for sterilization O/N. Then, MAEC were grown onto the BGs at a density of 2×10^4 cells cm^{-2} in a 24-well plate and cultured until 96 h. The suitable cell density, defined as the ratio of the number of cells for mg of bioglass, was set equal to 3000/mg.

At different time points (24 h, 48 h, 72 h, 96 h), cell viability was determined by the resazurin reduction assay as previously reported. At least three independent experiments were performed.

To assess the effects of the only ionic release on cell viability, the supernatant collected from granules cultured in DMEM for 48 h was employed as culture medium to grow the cells. Then, cell viability was assessed after 96 h by means of resazurin reduction assay, as previously done.

2.4. Phalloidin staining

The specimens were fixed with 4 % paraformaldehyde/PBS (Sigma Aldrich, Darmstadt, Germany), washed in 1× PBS, permeabilized with Triton-X 100 and labeled with TRITC-conjugated phalloidin (FAK100, Merck Millipore, Darmstadt, Germany) for 1 h, followed by several washing with 1 × PBS. Nuclei were counterstained with 4′,6-diamidino-2-phenylindole (DAPI, FAK100, Merck Millipore, Darmstadt, Germany) for 5 min, followed by several washing with 1xPBS. Samples were analyzed with a Nikon Eclipse 80i microscope equipped for fluorescence analysis (Nikon Instruments Europe BV, Amstelveen, The Netherlands) at different magnifications.

2.5. Reactive oxygen species (ROS)

For ROS evaluation the probe 20,70 -dichlorofluorescin-diacetate (H2DCF-DA) was used [28,29]. The cells were cultured on the three BGs with complete DMEM 10 % FBS for 96 h. After that time, 10 μM of H2DCF-DA were added to the for 30 min in the dark. Samples were observed under the same microscope mentioned above.

2.6. Scanning electron microscopy (SEM)

For SEM analysis, the specimens were treated as follows: immersed in 2.5 % glutaraldehyde/1xPBS at 4 °C overnight; then, rinsed 3 times in 1 × PBS for 5 min before being incubated for 1 h with 1 % osmium tetraoxide (OsO_4). The BGs were then rinsed 3 times with distilled water and dehydrated in an ascending ethanol series, then the specimens were air-dried, transferred over stubs and coated with a 10 nm thick gold layer by means of the Emitech K550 sputter coater (Quorum Technologies, South Stour Avenue, Kent, UK). BGs colonization was detected under high vacuum at the ESEM Quanta 200 SEM (Fei Company, Hillsboro, OR, USA) at different magnifications.

2.7. CAM assay

Fertilized Isa Brown chicken eggs (Commercial Farm Cellini Andrea, Forlì, Italy) were collected after the fertilization and incubated (FIEM Mercurius MG244, Como, Italy) at 48 % humidity and 37.8 °C temperature. As described in our protocol after 3 days of incubation and embryos development (ED3), following the Hamburger and Hamilton's classification, 3 mL of albumen were collected from one extremity of the eggshell to detach the developing CAM from the shell membrane [30]. Then, a small aperture was performed into the eggshell in order to verify embryos viability, right after sealed with 18 × 18 mm^2 coverslips and paraffin. At ED9 the bioactive glasses (45S5, BGMS10, Bio_MS), previously sterilized under UV light, were grafted onto the CAMs; opened and closed eggs without grafted materials were considered as control CAMs. For each experimental point, 6 eggs were exploited, and for these experiments at least three independent triplicates were performed. On the fourth day of incubation, which corresponds to ED13, the eggs were opened, and images from CAMs were taken *in ovo* employing a Nikon SMZ745T stereomicroscope (Nikon Instruments Europe BV, Amstelveen, The Netherlands) set with a digital camera and X-Entry software (both Alexasoft, Florence, Italy). Photographs were acquired at ED13 to monitor the vessel development around the BGs: the angiogenic reaction was assessed by comparing the grafted CAMs with the control CAMs at 1× magnification. For the angiogenic response evaluation, the vessel count was performed starting from the images of the CAMs at ED13; for each sample, the same round area surrounding the grafted materials was chosen. To evaluate the angiogenic response, WimCAM, a WIMASIS Image Software for CAM assays, was exploited. This tool analyzes the novel vessels developing radially from the grafted BGs, by exploring parameters such as the vessel density, the total vessel network length and the total branching points.

2.8. Histological analyses

The specimens (CAM with BGs) were fixed in PBS buffered 4 % paraformaldehyde, dehydrated with increasing ethanol concentrations, and methyl methacrylate (MMA) embedded (Sigma Aldrich, Milan, Italy). The specimens were cut in serial sections of 200 μm in thickness with a Leica SP 1600 microtome (Leica SpA, Milan, Italy) under water irrigation. The section thickness was reduced with emery papers and polishing was obtained with alumina. Then, samples were stained with the toluidine blue alcoholic solution for 2 min at 60 °C and rinsed with tap water. Images were acquired at 20× and 40× magnification using the same microscope mentioned above.

2.9. RNA extraction and quantitative real time-polymerase chain reaction (RT-qPCR)

For molecular studies, treated and control CAM samples were harvested at different time points (8 h and 48 h) to investigate the angiogenic reaction triggered by the BGs. In order to reduce the high variability intrinsic to this biological complex system, three CAM tissue samples were pooled together for each experimental point and three independent experiments were carried out. RNA extraction was performed using TRIzol™ Reagent (Invitrogen), following standard procedures. High-Capacity cDNA Reverse Transcription Kit (Thermo Fisher Scientific) was employed to obtain cDNA. Quantitative gene expression was assessed employing the TaqMan(R) Gene Expression Master Mix, using the QuantStudio1 Real-Time PCR (Thermo Fisher Scientific). The following chicken TaqMan probes were employed (all from Thermo Fisher Scientific): VEGF Receptor 2 (VEGFR2) (#Gg03346172_m1), Cadherin 5 (CDH5) (#Gg03364043_m1), Platelet Endothelial Cell Adhesion Molecule 1 (PECAM1) (#Gg03331692_m1), CD34 (#Gg07164057_g1). Glyceraldehyde 3-phosphate dehydrogenase (GAPDH) (#Gg03346982_m1) was employed as internal control. Relative quantification was calculated using the ΔΔCt method, and results

were plotted as $2^{-\Delta\Delta Ct}$.

2.10. Statistical analysis

Data from the angiogenic response evaluation and molecular analysis are expressed as mean ± standard deviation (SD). One-way ANOVA followed by Tukey's multiple comparison test was employed to evaluate significant differences among bioglasses. Significant p-values ($^{*}p < 0.05$, $^{**}p < 0.01$, $^{***}p < 0.001$) are detailed in figure legends. GraphPad Prism 5 (5.00 version software, San Diego, USA) was used for statistics and graphs. Fluorescence images were analyzed using ImageJ software (version 1.54 g; Wayne Rasband, National Institutes of Health, USA). The "Analyze Particles" function was used to quantify cell coverage, and statistical analysis was performed on a total of 100 individual granules for each bioactive glass formulation.

3. Results

3.1. Endothelial cells colonize the two novel BG formulations BGMS10 and Bio_MS and efficiently adhere and proliferate on their surfaces

Morphological analyses were firstly conducted to assess the capability of MAEC endothelial cells to adhere onto the glass surfaces. Fluorescence labeling of nucleus (DAPI) and F-actin filaments, which are pivotal in regulating cell functions such as proliferation, adhesion, differentiation and internal architecture, were investigated, indicating that MAEC cells were capable to colonize all the BGs surfaces, but to different extents. As shown in Fig. 1 a, MAEC homogeneously colonized BGMS10 and Bio_MS in all their three-dimensionality, whereas in 45S5 only a few widely dispersed cells were detected.

Quantitative surface coverage analysis revealed that MAECs covered only 10 % ± 2 % of the average grain area on 45S5, compared to 72 % ± 6 % on BGMS10 and 81 % ± 10 % on Bio_MS.

Moreover, the images at higher magnification indicated that MAEC efficiently attached to both novel formulations, showing their peculiar elongated morphology, whereas they displayed a round morphology over the gold standard 45S5 (Fig. 1a, b). This data was confirmed also by SEM analysis (Fig. 1c), which showed that MAEC were able to form different cell-to-cell interactions in BGMS10 and Bio_MS granules. Cells seemed to interact less effectively with the surface of 45S5, and an extensive deposition of calcium phosphate was evident, displaying a rounder morphology with fewer cell contacts. Thus, a more adherent cellular growth was also detected upon the novel formulations, compared to 45S5, where endothelial cells likely failed to show hexagonal dendritic shape, covered by depositions of spherical features. In addition, in 45S5 many debris were spotted over the material and near the cells. To explore the effects of BGs on cell proliferation, MAEC were seeded over the BGs and left to adhere and grow for 24 h, 48 h, 72 h, and 96 h. Results show that the two novel formulations, BGMS10 and Bio_MS, allowed a time dependent increase in cell viability compared to 45S5, which become significant at 72 h and 96 h of endothelial cell culture (Fig. 1d).

Lastly, reactive oxygen species (ROS) production was evaluated after seeding the cells for 96 h on the three different BGs, finding that in MAEC cells grown onto BGMS10 and Bio_MS the oxidative stress was significantly reduced, as shown in Fig. 1e. Overall, these data indicate that BGMS10 and Bio_MS were able to allow adhesion and cell proliferation better than 45S5, and that endothelial cells displayed a significant higher cell viability and less ROS production when cultured onto the novel BGs formulations, compared to cells grown upon 45S5 (Fig. 1).

3.2. BGMS10 and Bio_MS ionic release significantly impacts endothelial cell viability

The ion release profiles of 45S5, BGMS10 and Bio_MS were assessed after incubation of the glasses for 16 h, 48 h, 72 h, and 96 h in DMEM 10 % FBS to evaluate the differences among the three BGs analyzed. Comparing the BGs in the direct culture settings, the release of Ca ion appeared to be similar in 45S5 and BGMS10 with a time dependent increase, while Bio_MS Ca release was lower compared to the other BGs (Fig. 2a). After 16 h of incubation in complete DMEM, a significant greater release of Si ion was evident for the novel BGs compared to 45S5; in addition, after 48 h and 72 h of incubation, BGMS10 continued to release greater amounts of Si ions compared to the other BGs (Fig. 2c). Finally, at 96 h of incubation both BGMS10 and Bio_MS released a significant amount of Si ions compared to 45S5 (Fig. 2c).

The release of Mg and Sr ions from BGMS10 and Bio_MS was also assessed, demonstrating a significant higher and time dependent Mg release in Bio_MS compared to BGMS10, while the release of Sr ions in BGMS10 compared to Bio_MS did not reach significance (Fig. 2b, e). Regarding Na ions, after 48 h of incubation, it was evident that 45S5 released significantly greater amounts of sodium compared to the other novel BGs, maintaining this trend until 96 h of incubation in complete DMEM (Fig. 2d). Finally, to investigate the effect of the ionic release from bioactive glasses on endothelial cell viability, we performed a viability assay employing endothelial cells cultured in medium preconditioned for 72 h with each bioactive glass. Our results demonstrated that the cells grown in complete DMEM conditioned with BGMS10 and Bio_MS were significantly more viable compared to those cultured in complete DMEM conditioned with 45S5. These data indicate that the effects on cell proliferation are at least in part due to the ionic release from BGMS10 and Bio_MS (Fig. 2f).

3.3. BGMS10 and Bio_MS were able to induce a strong angiogenic response in ovo

To assess the *in vivo* angiogenic potential of BGMS10 and Bio_MS, we employed the Chorio-Allantoic Membrane (CAM) assay, an ethical model to simulate the *in vivo* conditions. At embryo development 9 (ED9) the bioactive glasses (45S5, BGMS10, Bio_MS) were grafted onto the CAMs (Fig. 3a); opened and closed eggs without grafted materials were considered as control CAMs (Fig. 3b, first image left).

After 4 days (ED 13), the vascular response initiated by the BG granules showed irregularly formed capillaries radiating outward from their center, resembling the spokes of a wheel (Fig. 3b). Further, many of these vessels branched dichotomously, a typical index of a strong angiogenic response in all bio-glasses analyzed. Firstly, our results confirmed that the three BGs employed were biocompatible [21,22,31]. Moreover, we observed an evident angiogenic potential of the BGs (with branched thin vessels exhibiting an irregular course) compared to the control CAMs (characterized by linear and regular thicker vessels forming the natural background of the membrane) (Fig. 3b). The angiogenic potential data revealed that all the BGs were significantly more pro-angiogenic than the control CAMs, in terms of both vessel density and total vessel network length (Fig. 3c). The vessel density considers the amounts of tubular structures in the entire image, expressed as percentage. The total vessel network length measures the complete length of the tubular structure in pixels. In addition, Bio_MS displayed a significantly higher total branching points (which represent parts of the tubular structure where three or more tubes can converge), compared to control CAMs (Fig. 3c).

3.4. Histological analyses showed in vivo remarkable cell proliferation and compatibility of BGs engrafted in CAM

The histological analysis of the control CAMs showed the typical structure with two superficial monolayered epithelia (the upper called chorionic, the lower allantoic) comprising an intermediate mesenchyme with wide blood vessels (CTRL in Fig. 4). The CAMs grafted with the granules displayed a remarkable proliferation of CAM tissues around the BGs compared to the controls, without visible inflammatory reactions. In particular, the toluidine blue staining revealed the presence of

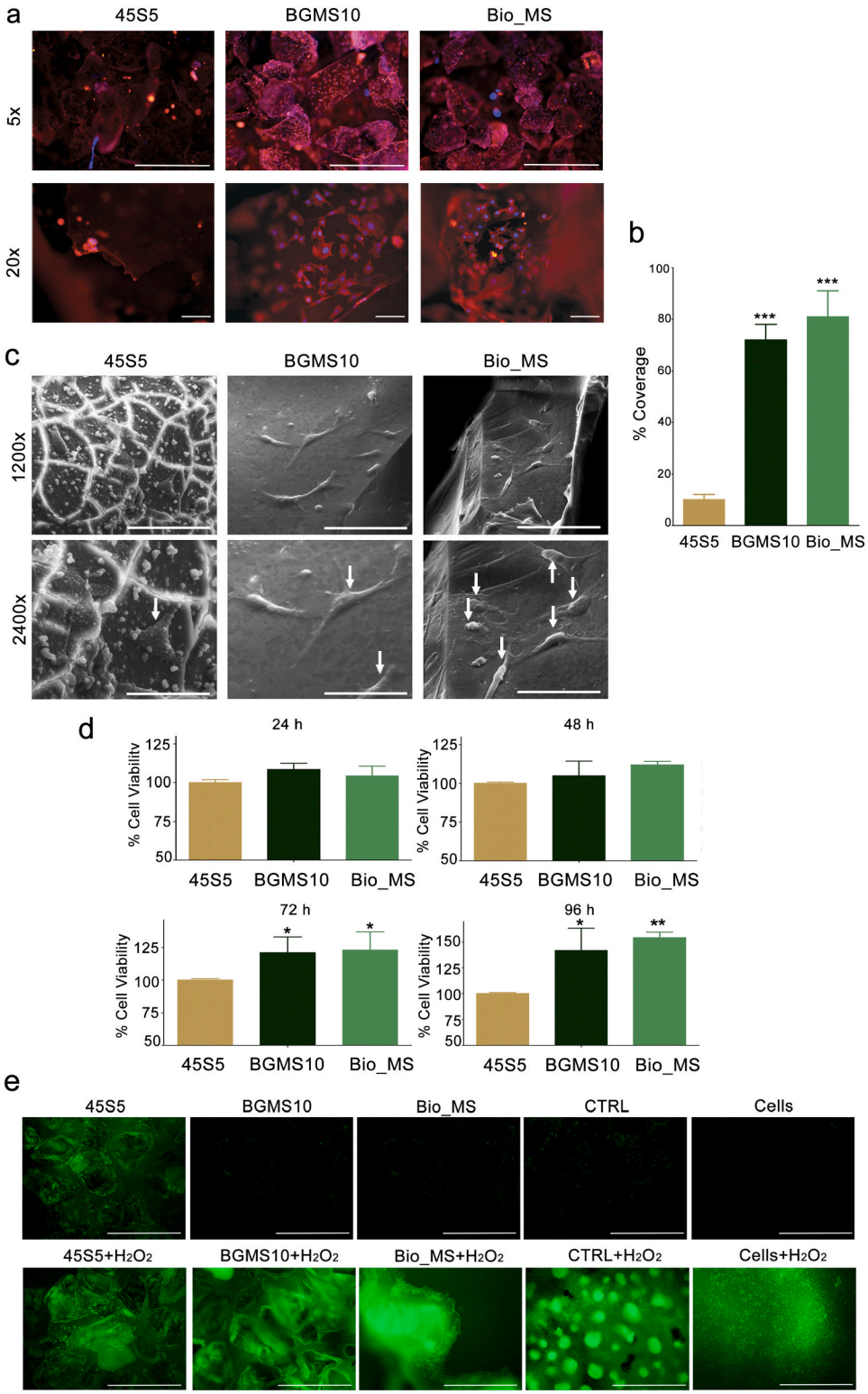

Fig. 1. Endothelial cells were able to colonize, to efficiently adhere and to proliferate on the surface of BGMS10 and Bio_MS a) Immunofluorescence analysis of MAEC colonization over the BG granules: cell nuclei in blue (DAPI), actin filaments in red (phalloidin staining); images were acquired at 5× (scale bar 1000 μm) and 20× magnification (scale bar 100 μm). b) Quantitative surface coverage analysis of MAEC cells on the three different BGs. Data were plotted as a percentage of coverage on the different BGs. Statistical analyses were performed using ANOVA. *** $p < 0.001$ denotes significant differences with respect to 45S5 c) Cell morphology of MAEC cells on the BGs was evaluated by SEM: the white arrows indicate the cells; magnification 1200× (scale bar 100 μm) and 2400× (scale bar 50 μm). d) Cell viability assays of MAEC endothelial cells cultured upon the three BGs granules. MAEC cell proliferation was assessed at 24 h, 48 h, 72 h and 96 h after seeding onto the BGs. Data were plotted as a percentage referred to 45S5. At least three independent experiments were performed. Statistical analyses were performed using ANOVA followed by Tukey's test. * $p < 0.05$, ** $p < 0.01$ denotes significant differences with respect to 45S5. e) ROS production of MAEC cells plated onto the 45S5, BGMS10, and Bio_MS BGs. Magnification 5×, scale bar 1000 μm.

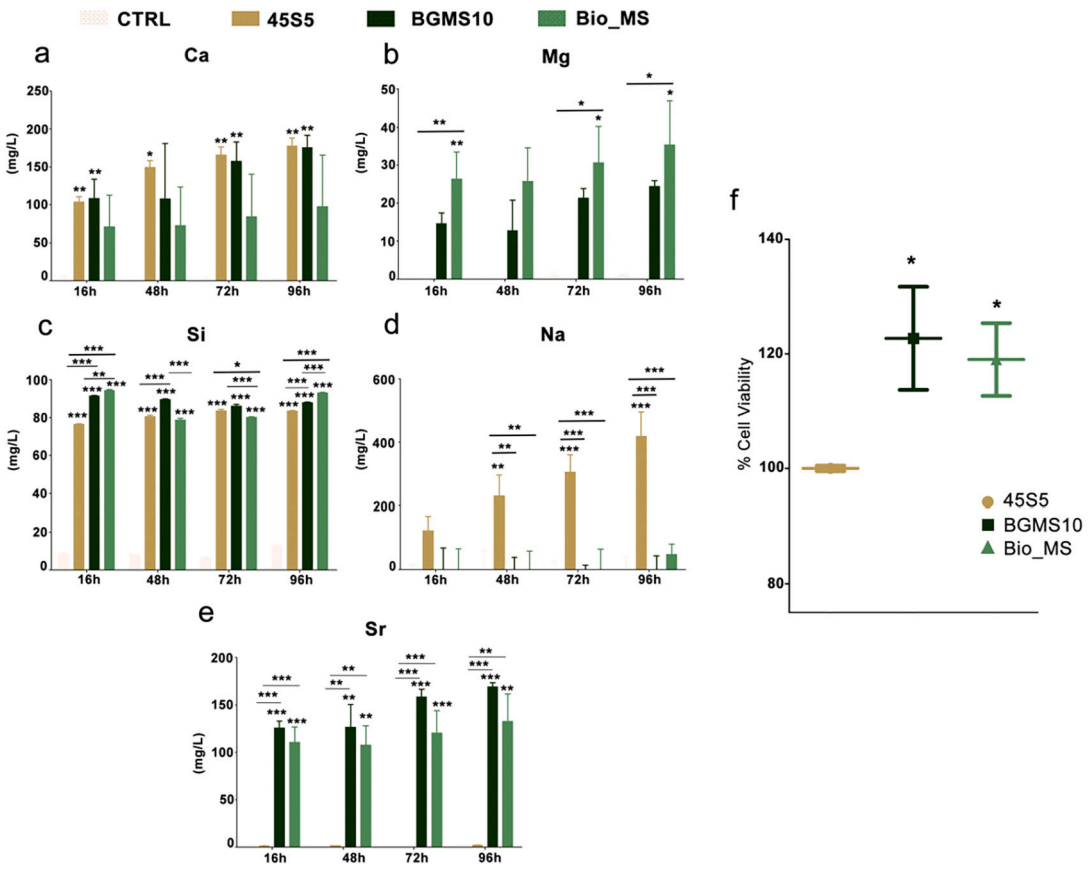

Fig. 2. Ionic release significantly affected endothelial cell viability. a, b, c, d, e) Ca, Mg, Si, Na, and Sr elemental concentrations (mg L^{-1}) were assessed by means of inductively coupled plasma (ICP) optical emission spectrometry of the three BGs after 16 h, 48 h, 72 h, and 96 h of incubation in DMEM 10 % FBS (complete). Statistical analyses were performed using one-way ANOVA with Bonferroni's correction: *$p < 0.005$; **$p < 0.01$; ***$p < 0.001$ denotes significant differences with respect to the control or the single bioglass when properly reported. f) Cell viability assays were performed by means of resazurin reduction assay. Cells were grown for 72 h in DMEM 10 % FBS previously conditioned with ions released from every single BG for 48 h. Data were plotted as a percentage referred to 45S5. At least three independent experiments were performed. Statistical analyses were performed using ANOVA followed by Tukey's test. *$p < 0.05$, **p < 0.01 denotes significant differences with respect to the control.

abundant connective tissue, rich in proteoglycans (as the metachromasia suggests) and vessels, mostly of small sizes, near the BGs. In addition, a neoformed multi-layered epithelium that encompasses the granules was also observed in the surrounding areas. Furthermore, the histological evaluation did not highlight any difference among the three BGs, confirming the results obtained with our previous analyses.

3.5. Vascular response is associated to a significant upregulation of genes involved in the angiogenic pathway

Since the BGs exhibited angiogenic response, gene expression analyses were conducted to deepen their biological activity at molecular level and to understand which genes could be involved in this process. To this aim, gene expression of *VEGFR2, CDH5, PECAM1* and *CD34* was evaluated by q*PCR* after 8 h and 48 h from the engraftment onto the CAM. We found no significant modulation after 8 h from the grafting, compared to control samples, which underwent the same treatment of other CAMs, without receiving the BGs (data not shown). Interestingly, an increase in gene expression of these pro-angiogenic markers was observed after 48 h from the grafting.

As reported in Fig. 5, *CDH5*, *CD34*, and *VEGFR2* expression was significantly upregulated in all the BGs. Moreover, the evaluation of the expression of *PECAM1* was assessed, due to its importance for endothelial cells. Our results showed no significant differences between 45S5 and BGMS10, compared to control, while the expression of *PECAM1* was significantly upregulated in tissues engrafted with Bio_MS (Fig. 5).

4. Discussion

Given the vital role that vascularization plays in effective bone regeneration, the restoration of a functional vascular network is a mandatory prerequisite for forming new matrices and inducing osteogenesis. Consequently, for an effective healing process, the angiogenic potential of biomaterials is essential for bone tissue engineering applications [23]. In this context, we analyzed the biocompatibility and the angiogenic potential of two novel BGs, BGMS10 and Bio_MS, tailored with magnesium and strontium (please refer to Table 1 for the composition), in both *in vitro* and *in ovo* settings. This choice was done due to the ameliorative properties of these ions in angiogenesis and bone regeneration. Indeed, previous findings have demonstrated that biomaterials containing Sr ions could promote angiogenesis. One example has been offered by the studies of Yan et colleagues, who demonstrated that applicable doses of Sr ions (0.2–1 mM) can boost the secretion of VEGFA and ANG-1 in endothelial cells and bone marrow stromal cells co-culture systems, which has the potential to create a favorable angiogenic microenvironment in the first stages of angiogenic process [32]. The experimental BG formulations here discussed were compared to the gold standard 45S5 Bioglass®, to assess their effects on endothelial cell adhesion, viability, proliferation, and in vascularization process. Firstly, we assessed the spreading rate of endothelial cells upon surface contact by examining the cell F-actin cytoskeleton. We found that the area engaged by the cell body during 45S5 cell adhesion was reduced compared to that of cells seeded on the new BGs. We also found

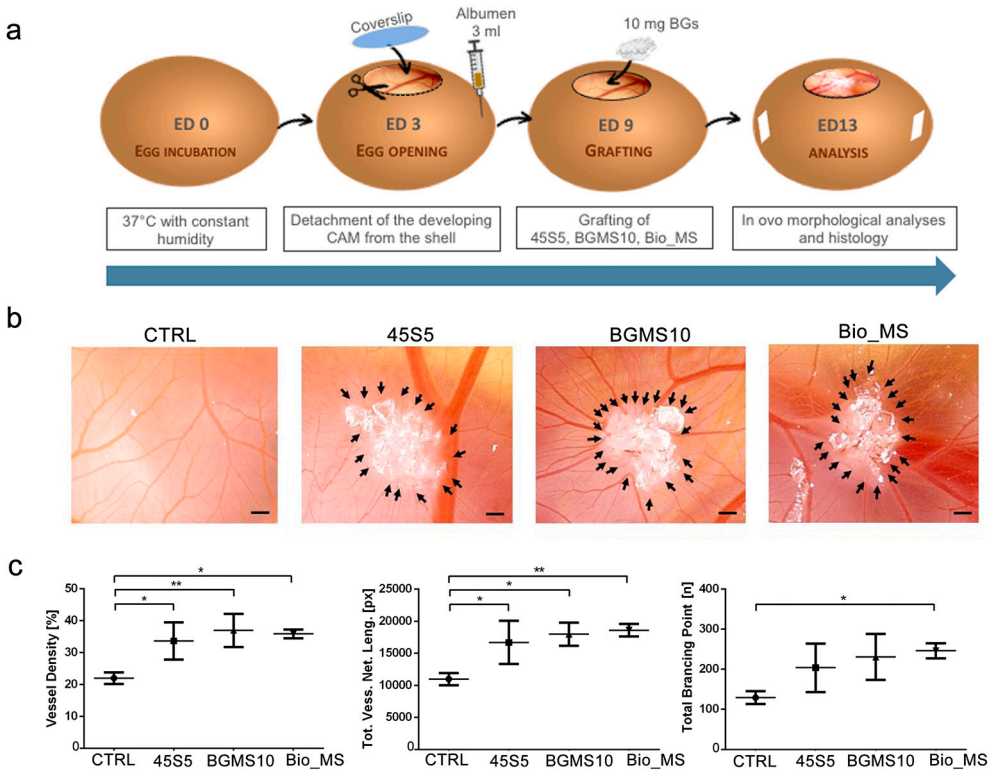

Fig. 3. CAM assay performed to test angiogenesis after the engraftment with 45S5, BGMS10, Bio_MS. a) Schematic representation of experimental design performed in ovo settings. b) Images taken at ED13, showing the vascular reaction triggered by the biomaterials after 4 days of engraftment with BGs; the black arrows indicate the vessels of neoformation sprouting radially from the BGs; magnification 1×, scale bar 250 μm. c) Angiogenic reaction was analyzed through the WimCAM software. The parameters analyzed were vessel density [%], total vessel network length [px] and total branching point [n]. Statistical analyses were performed employing one-way ANOVA with Tukey's correction for multiple comparisons (significance: $*p < 0.05$; $**p < 0.01$).

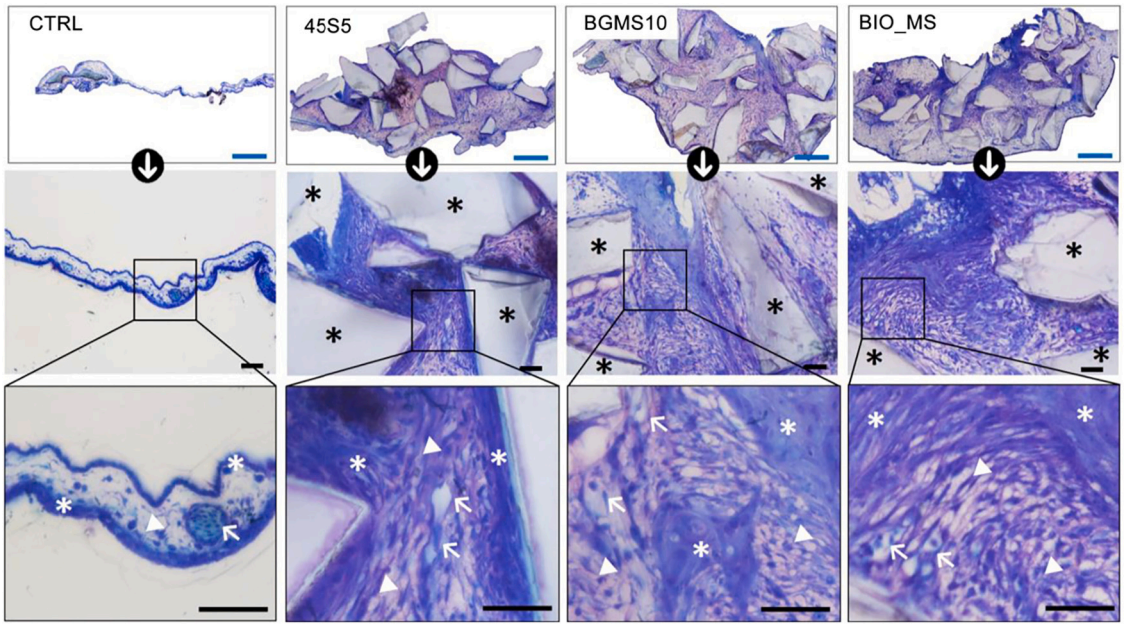

Fig. 4. Histological evaluation of BGs engraftment in CAM. Histological sections stained with toluidine blue of the control CAMs (CTRL) and the BG granules (black asterisks) grafted onto the CAMs; epithelial tissue in blue (white asterisks), connective tissue (arrow heads) with proteoglycans in purple, vessels (arrows); blue scale bar 500 μm, black scale bar 50 μm.

that endothelial cells were significantly more viable onto the surfaces of BGMS10 and Bio_MS, and maintained dendritic morphology, whereas cells cultured onto 45S5 displayed a round morphology, indicating a weaker attachment, accompanied by a significant release of reactive oxygen species, compared to the novel BGs formulations. Moreover, the stronger adhesion onto BGMS10 and Bio_MS allowed a time-dependent increase in cellular proliferation, compared to 45S5.

Interestingly, it is known that Mg absence or deficiency is related to

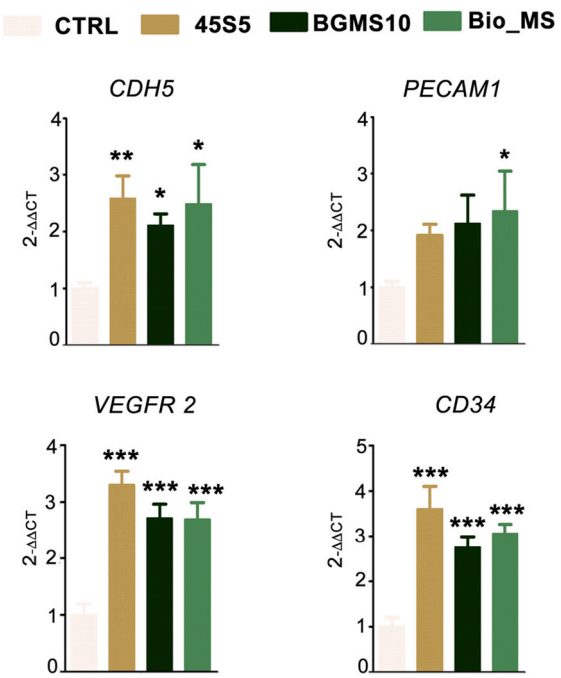

Fig. 5. CDH5, PECAM1, VEGFR2, and CD34 were significantly upregulated in tissues from CAM engrafted with BGs. Gene expression analyses were performed by means of RT-qPCR to assess the possible modulation of CDH5, CD34, PECAM1, and CD34. RNA was extracted from CAM tissues previously engrafted with the three BGs or control tissues. The data were normalized on the control CAMs and the endogenous gene GAPDH. At least three independent experiments were performed. Statistical analyses were performed employing one-way ANOVA (significance: $*p < 0.05$, $**p < 0.01$, $***p < 0.001$).

increased inflammatory responses, comprising the activation of leukocytes and macrophages, and additional ROS production [33]. In contrast, Mg ions can promote cell proliferation, migration, and osteogenic differentiation of BMSCs, and significantly influence angiogenesis by selectively activating the mitogen-activated protein kinase/extracellular signal-regulated kinase signaling cascades [19]. We observed a remarkable production of ROS in endothelial cells grown on 45S5 Bioglass®, while cells grown on the BGs doped with Mg were not affected.

To test the effects of the different chemical composition and the release of ions from BGs, the ion release profiles for Mg, Ca, Si, Sr and Na was assessed after incubation of 45S5, BGMS10 and Bio_MS, in complete DMEM (DMEM 10%FCS). We observed a significantly higher and time dependent Mg release in Bio_MS compared to BGMS10. The fact that Mg is released more in Bio_MS compared to BGMS10 is not surprising in terms of network connectivity (NC) [5]. In fact, the lower NC is, the more reactive the BG results, and if NC is above 2.6 the glass is no longer bioactive due to its resistance to dissolution [5]. Indeed, the NC of BGMS10 is 2.2, whereas NC is 2.1 in Bio_MS, explaining the difference between the two BGs in Mg release [34]. The effects of Mg release in increasing osteoblast proliferation and differentiation, as well as in enhancing expression of osteogenic markers – including osteopontin, osteocalcin, and osteonectin – in human bone derived cells were also documented [35–37]. Mg increased the expression of collagen type X and VEGF, enhanced matrix mineralization, and was beneficial for wound healing [38,39]. Remarkably, other recent works confirmed that the ionic release of both Mg and Sr improved both the angiogenic and the osteogenic effect of BGs, being in line with our results [40,41].

Lastly, we observed that 45S5 released great amounts of sodium ion, and this trend was maintained up to 96 h of incubation. It is known that this release can be dangerous for the cell viability and can cause cell death.

To further investigate the role of different ion concentrations in culture medium, we correlated the ionic release profiles of the three BGs with endothelial cell viability and proliferation, finding that cells incubated with medium conditioned from BGMS10 and Bio_MS were significantly more viable compared to those cultured with medium conditioned from 45S5 BG. These results can be explained, at least partially, by Na ions burst from 45S5, which drastically increased the local pH and induced ROS formation, likely favoring a precipitation environment for calcium and phosphate, as evidenced by the presence of cracks on 45S5 surface, indicative of amorphous calcium phosphate (ACP) formation and facilitated crystallization [42–45]. In our hands we observed a better adhesion, viability and proliferation of endothelial cells grown on BGMS10 and Bio_MS, compared to 45S5, likely due to a more favorable ionic release and better mechanical stability of the novel BGs.

Finally, we employed the CAM assay to assess the vascular growth potential of these novel materials, showing a significant evident vascular reaction for all BGs studied. However, none of the BG displayed significant differences in comparison to the other for the vessel density. This is in line with other studies which exploited the CAM assay to test 3D printed bioplastics, showing that different geometries of the same material displayed varying angiogenic responses onto the CAM [30]. These results likely indicate that CAM assay is reliable to assess if a specific geometry could be suitable to induce a vascular response. In this context, we found no differences between the 45S5 Bioglass® and the novel BGs employed. Among the three parameters that analyze the angiogenic response, the vessel density indicates a successfully angiogenic reaction onto the CAM, since it identifies the quantity of vessels close to the grafted materials and it represents a clear index of neoangiogenic response. Nevertheless, the total vessel network length and the branching points identify a “more mature” vascular network, which is subsequently developed, respectively representing the sum of the vessel's length and their points of intersection. For these parameters, we found that Bio_MS was more angiogenic compared to 45S5 and BGMS10, demonstrating a more established vascular network, in agreement with our *in vitro* results on cell viability.

To better assess the angiogenic reaction induced by the bioglasses, we performed histological analysis, finding that, compared to control CAMs, the toluidine blue staining evidenced abundant connective tissue rich in proteoglycans and a multi-layered epithelium surrounding the BGs. These results indicate that the granules had the ability to trigger a remarkable proliferation of the cells of the CAM tissues, highlighting the high biocompatibility of the BGs within biological systems. Additionally, the metachromasia indicated a possible osteo-inductive conditioning by means of osteochondral differentiation. These outcomes confirm what has already been observed in literature for the gold standard 45S5 Bioglass® [31]. We previously demonstrated that, under *in vivo* conditions, the 45S5 granules were predominantly encircled by broad and dispersed bone trabeculae separated by large amounts of soft tissue, which is a sign of poor mechanical properties. In contrast, around the two novel BG granules, the bone trabeculae were finer and evenly distributed. This latter finding could be considered more mechanically advantageous, since the two novel BG granules granted the formation of a uniform net of bone trabeculae, compared to 45S5 granules [46].

It is also interesting to note that the histology of the sections containing the granules showed the presence of vessels of neoformation in the proximity and among the BGs, easily recognizable for their smaller average size, in comparison to the ones of the CAM background, whose greater dimensions are visible in the control [47].

After the grafting with BG granules, we also evaluated expression of genes involved in angiogenic response. All evaluated genes were upregulated compared to control. In fact, even if the CAM model is not considered animal experimentation, its complexity and multi-tissue structuring could provide reliable outputs [48,49]. Specifically, we found that *VEGFR2,* which plays a key role in vascularization, was upregulated in all three BG analyzed [49]. In the CAM context, *VEGFR2* is in fact expected to be modulated when a pro-angiogenic biomaterial is

implanted, since the membrane reacts by forming new blood vessels around the graft. However, there were no significant differences between the three BG granules. As far as the analysis of cell-to-cell interaction is concerned, *CDH5*, also known as VE-cadherin, is a transmembrane protein associated with adherent junctions with a fundamental role in establishing functional cell-to-cell connections in endothelial cells forming the vessels. On the other hand, *PECAM1*, *i.e. CD31*, is a membrane glycoprotein, normally found on endothelial cells, which enables the formation of new blood vessels through cell-to-cell adhesions [50]. In our work, *CDH5* and *PECAM1* were evaluated to analyze the cell-to-cell connections that are fundamental for endothelial cells to assemble into new vessels. Our results indicate that all three BGs significantly triggered *CHD5* expression compared to control, while *PECAM1* expression was upregulated especially in tissue engrafted with Bio_MS. Collectively, these results suggest that all the BG granules may enhance cell-to-cell connections in CAM endothelial cells, and that Bio_MS could have better characteristics compared to the other BG granules. These findings are promising and surely warrant further investigation. Finally, *CD34* gene expression was evaluated, due to its role as stemness marker in hematopoietic stem and progenitor cells. In the context of vascularization, it is a surface glycoprotein expressed by quiescent endothelial cells at sites of active angiogenesis on the lumen of blood vessels [51]. The molecular analysis showed that the expression of *CD34* was higher compared to control CAM in all BG granules. These findings indicate that the quiescent endothelial stem cells were driven to massively proliferate by the BG granules, confirming the histological analyses. Overall, the results suggest that the BG granules were able to induce angiogenic processes through the upregulation of *VEGFR2* and *CD34*, and to enhance cell-to-cell connections in endothelial cells by means of *CDH5* and *PECAM1*.

5. Conclusions

The present study highlights the promising biological performance of two newly developed bioactive glass formulations, BGMS10 and Bio_MS, specifically designed to improve angiogenic potential and biocompatibility in the context of bone tissue regeneration. Compared to the conventional 45S5 Bioglass®, both BGMS10 and Bio_MS demonstrated enhanced bioactivity, supported by controlled and sustained release of key therapeutic ions such as Mg and Sr. These ions stimulated endothelial cell activity, reduce oxidative stress, and promoted angiogenesis in CAM models.

Importantly, the reduced Na release from BGMS10 and Bio_MS compared to 45S5 contributed to a more cytocompatible microenvironment, avoiding potential inflammatory responses and favoring endothelial activity. These findings position BGMS10 and Bio_MS as advanced materials with strong potential for regenerative applications. However, despite these advantages, the use of BG granules alone presents some limitations, particularly in load-bearing contexts where mechanical support is required. This issue opens up new design opportunities. In fact, the biological strengths of these materials make them excellent candidates for integration into composite scaffolds, wound dressings, dental putties, and coatings, as well as for aiding the repair of critical bone lesions which, due to their size and associated severe vascular damage, are unable to repair themselves.

Their high crystallization temperature further enhances their versatility in various processing techniques and biomedical formats. Finally, while current study provides robust evidence of bioactivity, further *in vivo* studies in large animal models are essential to validate their long-term regenerative capacity in clinically relevant defect environments.

Abbreviations

ACP	amorphous calcium phosphate
BG	bioactive glass
BMSC	bone marrow stromal cell
CAM	chorio-allantoic membrane
CDH5	Cadherin 5
DMEM	Dulbecco's Modified Eagle Medium
ED	embryos development
GAPDH	Glyceraldehyde 3-phosphate dehydrogenase
ICP	inductively coupled plasma
LOD	limit of detection
MAEC	mouse aortic endothelial cells
MMA	methyl methacrylate
MSC	human mesenchymal stem cell
NC	network connectivity
PBS	sodium phosphate-buffered
PDGF	platelet-derived growth factor
PECAM1	Platelet Endothelial Cell Adhesion Molecule 1
ROS	Reactive Oxygen Species
RSD	ratio of the standard deviation
SBF	simulated body fluid
SEM	scanning electron microscopy
VEGF-A	vascular endothelial growth factor A
VEGFR2	VEGF Receptor 2

CRediT authorship contribution statement

Marianna Barbalinardo: Writing – original draft, Methodology, Investigation, Data curation, Conceptualization. **Marzia Ferretti:** Writing – review & editing, Writing – original draft. **Virginia Stanzani:** Writing – original draft, Methodology, Investigation. **Francesca Chiarini:** Writing – review & editing, Writing – original draft, Validation, Supervision, Methodology, Data curation, Conceptualization. **Ilaria Zanoni:** Resources, Methodology, Investigation. **Francesca Paganelli:** Writing – review & editing, Investigation. **Marta Checchi:** Writing – review & editing, Methodology, Investigation. **Serena Truocchio:** Writing – review & editing, Investigation. **Matteo Corradini:** Investigation. **Vincenza Rita Lo Vasco:** Resources. **Francesco Cavani:** Writing – review & editing, Methodology. **Luca Reggiani Bonetti:** Methodology, Investigation. **Devis Bellucci:** Writing – review & editing, Resources, Methodology, Funding acquisition, Conceptualization. **Valeria Cannillo:** Writing – review & editing, Supervision, Resources, Conceptualization. **Carla Palumbo:** Supervision, Project administration, Funding acquisition.

Funding sources

Devis Bellucci received funds from Project FARD-2022 "MATLIFE", belonging to the Department of Engineering "Enzo Ferrari", University of Modena and Reggio Emilia, Modena, Italy. Carla Palumbo acknowledges that the work was funded with, provided by University of Modena and Reggio Emilia, and "Fondazione di Modena" (FOMO), Modena, Italy.

Declaration of competing interest

The authors declare the following financial interests/personal relationships which may be considered as potential competing interests: Devis Bellucci and Valeria Cannillo hold a patent for the bioactive glass Bio_MS (in granules): Italian patent No 102019000002229 dated February 15, 2019. The other authors declare that they have no known competing financial interests or personal relationships that could have appeared to influence the work reported in this paper.

Acknowledgements

The authors wish to thank Dr. Marta Benincasa for her support and technical assistance.

Data availability

The authors confirm that the data supporting the findings of this study are available within the article and its ESI.

References

[1] L.L. Hench, J.M. Polak, Third-generation biomedical materials, Science 295 (2002) 1014–1017, https://doi.org/10.1126/science.1067404.

[2] S. Pina, V.P. Ribeiro, C.F. Marques, F.R. Maia, T.H. Silva, R.L. Reis, J.M. Oliveira, Scaffolding strategies for tissue engineering and regenerative medicine applications, Materials (Basel) 12 (2019), https://doi.org/10.3390/ma12111824.

[3] Y. He, F. Lu, Development of synthetic and natural materials for tissue engineering applications using adipose stem cells, Stem Cells Int. 2016 (2016) 5786257, https://doi.org/10.1155/2016/5786257.

[4] M. Brovold, J.I. Almeida, I. Pla-Palacin, P. Sainz-Arnal, N. Sanchez-Romero, J. J. Rivas, H. Almeida, P.R. Dachary, T. Serrano-Aullo, S. Soker, P.M. Baptista, Naturally-derived biomaterials for tissue engineering applications, Adv. Exp. Med. Biol. 1077 (2018) 421–449, https://doi.org/10.1007/978-981-13-0947-2_23.

[5] J.R. Jones, Reprint of: review of bioactive glass: from Hench to hybrids, Acta Biomater. 23 (Suppl) (2015) S53–S82, https://doi.org/10.1016/j.actbio.2015.07.019.

[6] V. Miguez-Pacheco, L.L. Hench, A.R. Boccaccini, Bioactive glasses beyond bone and teeth: emerging applications in contact with soft tissues, Acta Biomater. 13 (2015) 1–15, https://doi.org/10.1016/j.actbio.2014.11.004.

[7] L. Lefebvre, J. Chevallier, L. Gremillard, R. Zenati, G. Thollet, D. Bernache-Assolant, A. Govin, Structural transformations of bioactive glass 45S5 with thermal treatments, Acta Mater. 55 (2007) 3305–3313, https://doi.org/10.1016/j.actamat.2007.01.029.

[8] A.A. Desoky, K.T. Ereiba, A.M. Bakr, A.S. Abdraboh, Enhancement of bioactivity and molecular docking analysis of bioglass loaded zein and sodium alginate composite beads for biomedical applications, Sci. Rep. 15 (2025) 13460, https://doi.org/10.1038/s41598-025-95691-7.

[9] Q. Yang, A. Chen, X. Zhang, Z. Wu, C. Zhang, Functional poly(ether-ketone-ketone) composite scaffold with enhanced cell-material interaction, anti-inflammatory and osteogenesis for facilitating osteointegration and bone regeneration, Mater Today Bio 31 (2025) 101533, https://doi.org/10.1016/j.mtbio.2025.101533.

[10] D. Dhinasekaran, G.S. Kaliaraj, M. Jagannathan, A.R. Rajendran, A. Prakasarao, S. Ganesan, B. Subramanian, Pulsed laser deposition of nanostructured bioactive glass and hydroxyapatite coatings: microstructural and electrochemical characterization, Mater. Sci. Eng. C Mater. Biol. Appl. 130 (2021) 112459, https://doi.org/10.1016/j.msec.2021.112459.

[11] D. Dhinasekaran, S. Vimalraj, A.R. Rajendran, S. Saravanan, B. Purushothaman, B. Subramaniam, Bio-inspired multifunctional collagen/electrospun bioactive glass membranes for bone tissue engineering applications, Mater. Sci. Eng. C Mater. Biol. Appl. 126 (2021) 111856, https://doi.org/10.1016/j.msec.2020.111856.

[12] D. Galuskova, H. Kankova, A. Svancarkova, D. Galusek, Early-stage dissolution kinetics of silicate-based bioactive glass under dynamic conditions: critical evaluation, Materials (Basel) 14 (2021), https://doi.org/10.3390/ma14123384.

[13] S. Gupta, S. Majumdar, S. Krishnamurthy, Bioactive glass: a multifunctional delivery system, J. Control. Release 335 (2021) 481–497, https://doi.org/10.1016/j.jconrel.2021.05.043.

[14] C. Blaeß, R. Müller, G. Poologasundarampillai, D.S. Brauer, Sintering and concomitant crystallization of bioactive glasses, Int. J. Appl. Glas. Sci. 10 (2019) 449–462, https://doi.org/10.1111/ijag.13477.

[15] D. Bellucci, V. Cannillo, A. Sola, Calcium and potassium addition to facilitate the sintering of bioactive glasses, Mater. Lett. 65 (2011) 1825–1827, https://doi.org/10.1016/j.matlet.2011.03.060.

[16] D. Bellucci, V. Cannillo, G. Ciardelli, P. Gentile, A. Sola, Potassium based bioactive glass for bone tissue engineering, Ceram. Int. 36 (2010) 2449–2453, https://doi.org/10.1016/j.ceramint.2010.07.009.

[17] H. Zhu, K. Zheng, A.R. Boccaccini, Multi-functional silica-based mesoporous materials for simultaneous delivery of biologically active ions and therapeutic biomolecules, Acta Biomater. 129 (2021) 1–17, https://doi.org/10.1016/j.actbio.2021.05.007.

[18] H. Li, J. Chang, Bioactive silicate materials stimulate angiogenesis in fibroblast and endothelial cell co-culture system through paracrine effect, Acta Biomater. 9 (2013) 6981–6991, https://doi.org/10.1016/j.actbio.2013.02.014.

[19] S. Kargozar, F. Baino, S. Hamzehlou, R.G. Hill, M. Mozafari, Bioactive glasses: sprouting angiogenesis in tissue engineering, Trends Biotechnol. 36 (2018) 430–444, https://doi.org/10.1016/j.tibtech.2017.12.003.

[20] D. Bellucci, V. Cannillo, A novel bioactive glass containing strontium and magnesium with ultra-high crystallization temperature, Mater. Lett. 213 (2018) 67–70, https://doi.org/10.1016/j.matlet.2017.11.020.

[21] D. Bellucci, E. Veronesi, V. Strusi, T. Petrachi, A. Murgia, I. Mastrolia, M. Dominici, V. Cannillo, Human mesenchymal stem cell combined with a new strontium-enriched bioactive glass: an ex-vivo model for bone regeneration, Materials (Basel) 12 (2019), https://doi.org/10.3390/ma12213633.

[22] D. Bellucci, E. Veronesi, M. Dominici, V. Cannillo, A new bioactive glass with extremely high crystallization temperature and outstanding biological performance, Mater. Sci. Eng. C Mater. Biol. Appl. 110 (2020) 110699, https://doi.org/10.1016/j.msec.2020.110699.

[23] S. Stegen, N. van Gastel, G. Carmeliet, Bringing new life to damaged bone: the importance of angiogenesis in bone repair and regeneration, Bone 70 (2015) 19–27, https://doi.org/10.1016/j.bone.2014.09.017.

[24] M. Checchi, V. Stanzani, S. Truocchio, M. Corradini, M. Ferretti, C. Palumbo, From morphological basic research to proposals for regenerative medicine through a translational perspective, Ital. J. Anat. Embryol. 126 (2022) 139–145, https://doi.org/10.36253/ijae-13727.

[25] D. Ribatti, Two new applications in the study of angiogenesis the CAM assay: acellular scaffolds and organoids, Microvasc. Res. 140 (2022) 104304, https://doi.org/10.1016/j.mvr.2021.104304.

[26] C.S. Kue, K.Y. Tan, M.L. Lam, H.B. Lee, Chick embryo chorioallantoic membrane (CAM): an alternative predictive model in acute toxicological studies for anti-cancer drugs, Exp. Anim. 64 (2015) 129–138, https://doi.org/10.1538/expanim.14-0059.

[27] D. Bellucci, R. Salvatori, A. Anesi, L. Chiarini, V. Cannillo, SBF assays, direct and indirect cell culture tests to evaluate the biological performance of bioglasses and bioglass-based composites: three paradigmatic cases, Mater. Sci. Eng. C 96 (2019) 757–764, https://doi.org/10.1016/j.msec.2018.12.006.

[28] S.F. Rapa, B. Waltenberger, R. Di Paola, S. Adesso, R. Siracusa, A.F. Peritore, R. D'Amico, G. Autore, S. Cuzzocrea, H. Stuppner, S. Marzocco, Plumericin prevents intestinal inflammation and oxidative stress in vitro and in vivo, FASEB J. 34 (2020) 1576–1590, https://doi.org/10.1096/fj.201902040R.

[29] H. Wang, J.A. Joseph, Quantifying cellular oxidative stress by dichlorofluorescein assay using microplate reader, Free Radic. Biol. Med. 27 (1999) 612–616, https://doi.org/10.1016/s0891-5849(99)00107-0.

[30] V. Stanzani, A. Giubilini, M. Checchi, F. Bondioli, M. Messori, C. Palumbo, Eco-sustainable approaches in bone tissue engineering: evaluating the Angiogenic potential of different poly(3-Hydroxybutyrate-co-3-Hydroxyhexanoate)–Nanocellulose composites with the Chorioallantoic membrane assay, Adv. Eng. Mater. 25 (2023) 2200934, https://doi.org/10.1002/adem.202200934.

[31] L.L. Hench, The story of bioglass, J. Mater. Sci. Mater. Med. 17 (2006) 967–978, https://doi.org/10.1007/s10856-006-0432-z.

[32] R. Yan, J. Li, Q. Wu, X. Zhang, L. Hu, Y. Deng, R. Jiang, J. Wen, X. Jiang, Trace element-augmented titanium implant with targeted angiogenesis and enhanced Osseointegration in osteoporotic rats, Front. Chem. 10 (2022) 839062, https://doi.org/10.3389/fchem.2022.839062.

[33] R. Van Orden, D.L. Eggett, K.B. Franz, Influence of graded magnesium deficiencies on white blood cell counts and lymphocyte subpopulations in rats, Magnes. Res. 19 (2006) 93–101.

[34] A. Pedone, V. Cannillo, M.C. Menziani, Toward the understanding of crystallization, mechanical properties and reactivity of multicomponent bioactive glasses, Acta Mater. 213 (2021) 1359–6454, https://doi.org/10.1016/j.actamat.2021.116977.

[35] A. Hoppe, N.S. Guldal, A.R. Boccaccini, A review of the biological response to ionic dissolution products from bioactive glasses and glass-ceramics, Biomaterials 32 (2011) 2757–2774, https://doi.org/10.1016/j.biomaterials.2011.01.004.

[36] R. Wetzel, M. Blochberger, F. Scheffler, L. Hupa, D.S. Brauer, Mg or Zn for ca substitution improves the sintering of bioglass 45S5, Sci. Rep. 10 (2020) 15964, https://doi.org/10.1038/s41598-020-72091-7.

[37] S.M. Rabiee, N. Nazparvar, M. Azizian, D. Vashaee, L. Tayebi, Effect of ion substitution on properties of bioactive glasses: a review, Ceram. Int. 41 (2015) 7241–7251, https://doi.org/10.1016/j.ceramint.2015.02.140.

[38] E. O'Neill, G. Awale, L. Daneshmandi, O. Umerah, K.W.-H. Lo, The roles of ions on bone regeneration, Drug Discov. Today 23 (2018) 879–890, https://doi.org/10.1016/j.drudis.2018.01.049.

[39] T. Mehrabi, A.S. Mesgar, Z. Mohammadi, Bioactive glasses: a promising therapeutic ion release strategy for enhancing wound healing, ACS Biomater Sci. Eng. 6 (2020) 5399–5430, https://doi.org/10.1021/acsbiomaterials.0c00528.

[40] V.M. Schatkoski, T.L. do Amaral Montanheiro, B.R. Canuto de Menezes, R. M. Pereira, K.F. Rodrigues, R.G. Ribas, D. Morais da Silva, G.P. Thim, Current advances concerning the most cited metal ions doped bioceramics and silicate-based bioactive glasses for bone tissue engineering, Ceram. Int. 47 (2021) 2999–3012, https://doi.org/10.1016/j.ceramint.2020.09.213.

[41] V. Mouriño, R. Vidotto, J.P. Cattalini, A.R. Boccaccini, Enhancing biological activity of bioactive glass scaffolds by inorganic ion delivery for bone tissue engineering, Curr. Opin. Biomed. Eng. 10 (2019) 23–34, https://doi.org/10.1016/j.cobme.2019.02.002.

[42] V. Sugumaran, A.J. Pavithra, B. Purushothaman, B. Subramanian, Crucial chemical revelations in 45S5 bioactive glass via sequential precursor integration order, ACS Appl Bio Mater 7 (2024) 1600–1620, https://doi.org/10.1021/acsabm.3c01099.

[43] V. Sugumaran, E. Krishnamoorthy, A. Kamalakkannan, R.C. Ramachandran, B. Subramanian, Unscrambling the influence of sodium cation on the structure, bioactivity, and erythrocyte compatibility of 45S5 bioactive glass, ACS Appl. Bio Mater. 5 (2022) 1576–1590, https://doi.org/10.1021/acsabm.1c01322.

[44] S.I. Schmitz, B. Widholz, C. Essers, M. Becker, D.U. Tulyaganov, A. Moghaddam, I. Gonzalo de Juan, F. Westhauser, Superior biocompatibility and comparable osteoinductive properties: sodium-reduced fluoride-containing bioactive glass belonging to the CaO-MgO-SiO(2) system as a promising alternative to 45S5 bioactive glass, Bioact Mater 5 (2020) 55–65, https://doi.org/10.1016/j.bioactmat.2019.12.005.

[45] S. Tsitlakidis, F. Hohenbild, M. Saur, A. Moghaddam, E. Kunisch, T. Renkawitz, I. Gonzalo de Juan, F. Westhauser, Reduced sodium portions favor osteogenic properties and Cytocompatibility of 45S5-based bioactive glass particles, Biomimetics (Basel) 8 (2023), https://doi.org/10.3390/biomimetics8060472.

[46] A. Anesi, M. Ferretti, R. Salvatori, D. Bellucci, F. Cavani, M. Di Bartolomeo, C. Palumbo, V. Cannillo, In-vivo evaluations of bone regenerative potential of two

novel bioactive glasses, J. Biomed. Mater. Res. A 111 (2023) 1264–1278, https://doi.org/10.1002/jbm.a.37526.
[47] D. Ribatti, B. Nico, A. Vacca, L. Roncali, P.H. Burri, V. Djonov, Chorioallantoic membrane capillary bed: a useful target for studying angiogenesis and anti-angiogenesis in vivo, Anat. Rec. 264 (2001) 317–324, https://doi.org/10.1002/ar.10021.
[48] D. Fischer, G. Fluegen, P. Garcia, N. Ghaffari-Tabrizi-Wizsy, L. Gribaldo, R. Y. Huang, V. Rasche, D. Ribatti, X. Rousset, M.T. Pinto, J. Viallet, Y. Wang, R. Schneider-Stock, The CAM model-q&a with experts, Cancers (Basel) 15 (2022), https://doi.org/10.3390/cancers15010191.
[49] A. Gheorghescu, J. Thompson, Delayed vasculogenesis and impaired angiogenesis due to altered Ang-2 and VE-cadherin levels in the chick embryo model following exposure to cadmium, Pediatr. Surg. Int. 32 (2016) 175–186, https://doi.org/10.1007/s00383-015-3830-9.
[50] H.M. DeLisser, M. Christofidou-Solomidou, R.M. Strieter, M.D. Burdick, C. S. Robinson, R.S. Wexler, J.S. Kerr, C. Garlanda, J.R. Merwin, J.A. Madri, S. M. Albelda, Involvement of endothelial PECAM-1/CD31 in angiogenesis, Am. J. Pathol. 151 (1997) (1997) 671–677.
[51] M.J. Siemerink, I. Klaassen, I.M. Vogels, A.W. Griffioen, C.J. Van Noorden, R. O. Schlingemann, CD34 marks angiogenic tip cells in human vascular endothelial cell cultures, Angiogenesis 15 (2012) 151–163, https://doi.org/10.1007/s10456-011-9251-z.